Tetrahedron 64 (2008) 8630–8637

Contents lists available at ScienceDirect

Tetrahedron

journal homepage: www.elsevier.com/locate/tet

Conformational reactions of D_2-symmetric twisted acenes

Robert A. Pascal, Jr. *, Qian Qin

Department of Chemistry, Princeton University, Princeton, NJ 08544, USA

ARTICLE INFO

Article history:
Received 29 March 2008
Received in revised form 7 May 2008
Accepted 8 May 2008
Available online 11 May 2008

Keywords:
Polycyclic aromatic hydrocarbons
Acenes
Conformational analysis
Transition state analysis
Dynamic NMR spectroscopy

ABSTRACT

Computational analyses of the longitudinally twisted polycyclic aromatic hydrocarbons 9,18-diphenyltetrabenz[*a*,*c*,*h*,*j*]anthracene (**1**), 9,10,19,20-tetraphenyltetrabenzo[*a*,*c*,*j*,*l*]naphthacene (**2**), and 9,10,11,20,21,22-hexaphenyltetrabenzo[*a*,*c*,*l*,*n*]pentacene (**3**) were performed at the B3LYP/6-31G(d) level of theory. Ground state and transition state structures were located for two classes of conformational reactions in these molecules: twist inversions (enantiomerization or racemization reactions) and phenyl rotations, and the free energies of activation for these processes were calculated. Where possible, the computational results were compared with both new and existing experimental data for the rates of these conformational reactions. Multiple pathways were identified for some processes, but the low-energy transition states were often quite different from those that common chemical intuition might suggest.

© 2008 Elsevier Ltd. All rights reserved.

1. Introduction

The typical acene is a flat, linear chain of fused benzene rings, but one need only attach a few bulky substituents to such a molecule and substantial deformations from planarity may result, most commonly in the form of a twisting distortion.[1] Thus, while anthracene and pentacene are flat, 9,18-diphenyltetrabenz[*a*,*c*,*h*,*j*]anthracene (**1**) and 9,10,11,20,21,22-hexaphenyltetrabenzo[*a*,*c*,*l*,*n*]pentacene (**3**) are twisted ribbons. In the solid state, they adopt conformations of approximate D_2 symmetry with end-to-end twists of 66° and 144°, respectively, and various computational studies indicate that D_2-symmetric, twisted conformations are the ground state structures in the gas phase as well.[2–6] These two polyphenyl tetrabenzoacenes, along with 9,10,19,20-tetraphenyltetrabenzo[*a*,*c*,*j*,*l*]naphthacene (**2**),[7] are the paradigmatic twisted acenes.

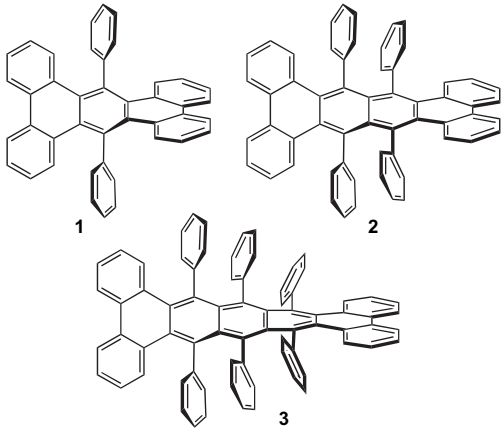

Compounds **1**–**3** are obviously chiral, but they have disappointingly low barriers to racemization. For **1**, the free energy of activation for this process ($\Delta G^{\ddagger}_{rac}$) is estimated to be 16.7 kcal/mol based on dynamic NMR studies of a diisopropyl derivative,[3] and such a low barrier precludes the resolution of enantiomers above −60 °C. Compound **3** *has* been resolved by chiral chromatography, but it racemizes with a half-life of 9.3 h at 25 °C ($\Delta G^{\ddagger}_{rac}$=23.8 kcal/mol).[4,5] For comparison, the helicenes typically have high barriers to racemization ($\Delta G^{\ddagger}_{rac}$=35–44 kcal/mol[8]). It has always been clear that the twisted acenes do not racemize via a single, planar transition state; such a process would have high activation energy. Instead, the twists must invert via lower energy, nonplanar intermediates and transition states. In this paper we explore the pathways for twist inversion (enantiomerization) of compounds **1**–**3**, as well as phenyl rotation reactions in these molecules, by means of computational studies at the B3LYP/6-31G(d) level of theory. The study of these highly symmetric molecules might be easier, both computationally and experimentally, than that of less symmetric twisted compounds, because the former have fewer conformations to evaluate and simpler spectra. Nonetheless, compounds **1**–**3**, though quite similar in appearance, proved to be remarkably different in their conformational dynamics.

* Corresponding author. Tel.: +1 609 258 5417; fax: +1 609 258 6746.
E-mail address: snake@chemvax.princeton.edu (R.A. Pascal Jr.).

0040-4020/$ – see front matter © 2008 Elsevier Ltd. All rights reserved.
doi:10.1016/j.tet.2008.05.030

Table 1
Calculated energies for conformations and conformational transition states of compounds **1**–**3** at the B3LYP/6-31G(d) level of theory

Conformation	Symm.	ΔE	ΔE_{corr}	ΔG_{298}	n_I	ν_{min}	$\Delta G^{\ddagger}_{expt}$ (T)
*Compound **1***							
Ground state	D_2	0.0	0.0	0.0	0	25.2	
Highest possible symmetry	D_{2h}	37.3	37.3	42.1	5	−114.1	
Twist inversion TS	C_{2h}	17.8	17.5	18.2	1	−13.4	16.7 (300 K)[b]
'Slice' conformation	C_{2h}	24.1	24.0	22.2	0	18.0	
'Butterfly' TS	C_{2v}	28.5	27.8	27.7	1	−17.4	
Phenyl rotation TS	C_2	37.4	36.7	36.7	1	−92.3	
Inversion-rotation TS	C_s	22.8	22.4	21.4	1	−30.0	19.2 (348 K)[c]
*Compound **2***							
Ground state	D_2	0.0	0.0	0.0	0	18.3	
Highest possible symmetry	D_{2h}	78.5	78.9	87.2	7	−135.4	
Twist inversion TS1	C_1	21.2	21.3	21.2	1	−27.3	
Twist inversion INT1	C_2	20.7	20.9	19.9	0	14.9	
Twist inversion TS2	C_1	21.9	22.0	22.0	1	−13.6	
Twist inversion INT2	C_1	21.6	21.9	20.5	0	10.9	
Twist inversion TS3	C_1	25.5	25.8	26.6	1	−25.9	
Twist inversion INT3	C_i	22.4	22.5	21.4	0	12.2	
Phenyl rotation TS	C_1	37.4	37.1	36.5	1	−104.9	
*Compound **3***							
Ground state	D_2	0.0	0.0	0.0	0	12.0	
Highest possible symmetry	D_{2h}	135.8	136.3	153.0	11	−148.5	
Twist inversion TS1	C_1	29.9	30.6	33.2	1	−13.6	23.8 (298 K)[d]
Twist inversion INT	C_2	19.3	19.9	20.5	0	14.2	
Twist inversion TS2	C_{2h}	19.5	19.9	20.9	1	−13.2	
Central phenyl rotation TS	C_1	36.9	36.9	37.0	1	−75.9	
Side phenyl rotation TS	C_1	35.8	35.6	35.5	1	−103.3	

For each entry, the energy relative to the D_2 ground state (ΔE, kcal/mol), the zero-point-corrected relative energy [$\Delta E_{corr}=\Delta(E+ZPE)$], the relative free energy (ΔG_{298}), the number of imaginary frequencies (n_I), and the lowest calculated frequency (ν_{min}, cm^{-1}) are given.[a] The experimental free energies of activation for the conformational reactions corresponding to the calculated transition states, where known, are given in the last column.

[a] The calculated absolute energies (E, E_{corr}, and G_{298}) are found in Supplementary data.

[b] Ref. 3.

[c] This work.

[d] Ref. 5.

2. Results and discussion

2.1. Twist inversion in 9,18-diphenyltetrabenz[*a,c,h,j*]anthracene (1)

The crystal structure of compound **1** as well as those of two simple derivatives show molecules with approximate D_2 symmetry and end-to-end twists of 61–70°,[2,3] and these findings are well reproduced by molecular mechanics (Sybyl,[9] MMFF[10]), semi-empirical (AM1[11]), ab initio (HF/STO-3G, HF/3-21G[12]), and density functional [B3LYP/6-31G(d)[13,14]] calculations.

A frequency calculation for the B3LYP/6-31G(d) structure shows it to be a potential energy minimum (0 imaginary frequencies; see Table 1), and extensive computational searches have failed to find a lower energy conformation. Given these data, the D_2 conformation may safely be taken to be the ground state of **1**.

A naïve analysis might suggest that the transition state for the twist inversion would be a D_{2h}-symmetric structure with a flat tetrabenzanthracene core. Such a structure possesses the highest symmetry that compound **1** might attain. However, geometry optimization of this D_{2h} structure followed by a frequency calculation shows it to be a saddle point of order 5 lying 42.1 kcal/mol above the ground state (Table 1).[15] Thus D_{2h}-**1** is chemically irrelevant, and at least some reduction of the symmetry is necessary to locate the true transition state structure.

The correct potential energy profile (Fig. 1) for the twist inversion of compound **1** proved to be quite simple, at least at the B3LYP/6-31G(d) level of theory. Geometry optimization of a wave-like, C_{2h}-symmetric structure for **1** yields a genuine transition state (TS, Fig. 1) for the twist inversion that lies 18.2 kcal/mol above the ground states (GS and eGS, for 'ground state' and 'enantiomeric ground state'). This TS structure displays a single imaginary frequency, and when small distortions are applied to reduce the symmetry to C_2, it rapidly evolves to the GS upon geometry optimization. Further, the calculated barrier for this structure is in good agreement with the experimental value for the enantiomerization of **1** (16.7 kcal/mol[3]).

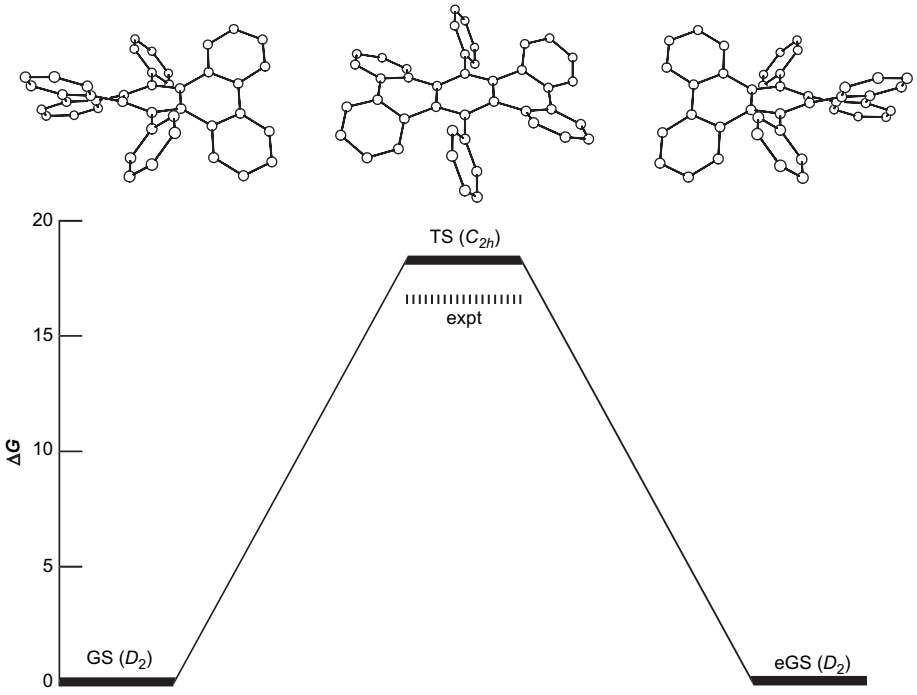

Figure 1. Free energy profile for the twist inversion of 9,18-diphenyltetrabenz[*a,c,h,j*]anthracene (**1**) calculated at the B3LYP/6-31G(d) level of theory. The ball-and-stick drawings illustrate the potential minima and transition state structures for this process.

This simple picture is pleasing, but it is important to note that the structures illustrated in Figure 1 are not the *only* minima and transition states potentially available to compound **1**, even if one limits the possibilities to structures that might be involved in twist inversion. For example, the next lowest energy minimum located for **1** is the C_{2h}-symmetric 'slice' conformation (below left). As an achiral structure, it is a candidate intermediate for the twist inversion, but its relative energy is 22.2 kcal/mol above the GS and thus this conformation is probably unimportant. There are also alternative TS structures for twist inversion. The C_{2v}-symmetric 'butterfly' structure (below right) *is* a genuine enantiomerization TS. It has one imaginary frequency, and slight distortions give a C_2 'butterfly' structure that is smoothly converted to the GS upon geometry optimization. Unfortunately, this C_{2v}-TS is 27.7 kcal/mol above the GS, and cannot compete with the wavelike C_{2h} TS that is almost 10 kcal/mol lower in energy. Surprisingly, however, this C_{2v} geometry is chemically significant: exactly this conformation has been observed in the X-ray crystal structure of the dilithium dianion of compound **1**.[16]

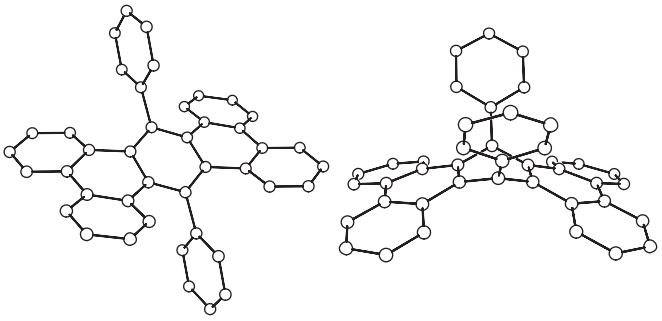

2.2. Twist inversion in 9,10,19,20-tetraphenyltetrabenzo[*a,c,j,l*]naphthacene (2)

A previous molecular mechanics study indicated that compound **2** has a D_2-symmetric ground state, but unlike compounds **1** and **3**, there is no crystal structure of **2**.[7] At both the AM1 and B3LYP/6-31G(d) levels of theory, D_2-**2** is the lowest energy conformation, and the end-to-end twist is calculated to be 109.4° at the latter level. All attempts to resolve compound **2** by chiral chromatography have been unsuccessful, but this does not necessarily indicate that the barrier to racemization is low. Computational studies have the potential to clarify this issue.

The enantiomerization of compound **2** was examined first at the AM1 level, and it was soon obvious that the reaction path was unusually complex and populated by numerous shallow minima and low transition states. The structures resulting from that study (not shown) were then used as starting points for the B3LYP/6-31G(d) calculations that ultimately led to the reaction profile illustrated in Figure 2. Two symmetric structures were initially identified as likely candidates for intermediates on the racemization pathway: the C_2-symmetric INT1 (ΔG=19.9 kcal/mol) and the C_i-symmetric INT3 (ΔG=21.4 kcal/mol). The difficult task was linking these structures by well-defined transition states and intermediates to the D_2 GS.

The first barrier to racemization is provided by TS1 (ΔG=21.2 kcal/mol). In this structure, benzo group A (see Fig. 2) has already moved past the adjacent phenyl ring, and benzo group B is in mid-pass relative to its neighboring phenyl; completion of this movement gives the C_2 INT1. So far the reaction path is clear, but no single transition state has been found to lead directly from INT1 to INT3. Instead, it is necessary to rotate one of the phenyl groups in INT1 by roughly 90° to give the closely related INT2 (ΔG=20.5 kcal/

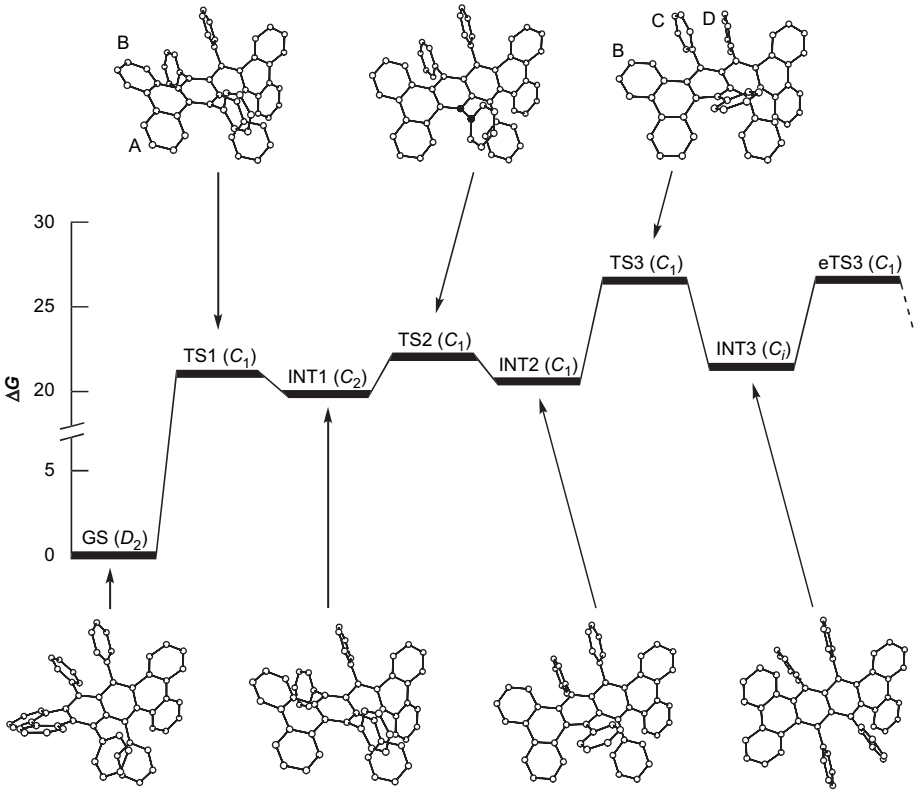

Figure 2. Free energy profile for the twist inversion of 9,10,19,20-tetraphenyltetrabenzo[*a,c,j,l*]naphthacene (**2**) calculated at the B3LYP/6-31G(d) level of theory. The ball-and-stick drawings below the profile illustrate the potential minima, and the drawings above illustrate the transition state structures for this process. Only half of the free energy profile is shown; the potential minima and transition states following INT3 are the enantiomers of those illustrated.

mol) via the modest TS2 (ΔG=22.0 kcal/mol); rotation occurs about the bond denoted by solid atoms in Figure 2. After many trials using the quadratic synchronous transit search algorithms (QST2 and QST3) in GAUSSIAN 03, a transition state (TS3, ΔG=26.6 kcal/mol) was found to link INT2 and INT3. Animation of the imaginary mode in TS3 reveals a complex motion in the transition state: benzo group B is moving past phenyl C while phenyls C and D are moving in the opposite direction. When small distortions are applied to the TS3 structure, it evolves smoothly into INT2 or INT3 upon geometry optimization, as expected. Once INT3 is attained, racemization is completed via enantiomeric transition states and intermediates that lead to the enantiomeric ground state.

TS3 is the rate limiting transition state for racemization of **2**. It is 26.6 kcal/mol above the ground state, suggesting that the enantiomers of **2** should be configurationally stable at room temperature. However, in a prior study of a complex polyphenylene, we found that B3LYP/6-31G(d) overestimated conformational barriers by an average of 3 kcal/mol.[17] We suspect, then, that the true barrier for the enantiomerization of **2** is no greater than 24 kcal/mol, making it potentially resolvable, but not configurationally stable at room temperature.

2.3. Twist inversion in 9,10,11,20,21,22-hexaphenyltetrabenzo[*a*,*c*,*l*,*n*]pentacene (3)

As observed for compound **1**, the X-ray crystal structures of **3** and a dimethyl derivative show that the molecules adopt conformations with approximate D_2 symmetry and end-to-end twists of 138–144°,[4,5] and a D_2 GS is also indicated by calculations at several levels of theory.[4–6] We have previously reported AM1 calculations indicating that the enantiomeric D_2 ground states of **3** interconvert via a C_{2h}-symmetric intermediate, by means of enantiomeric C_1-symmetric transition states lying 23.0 kcal/mol above the GS, in excellent agreement with the experimental $\Delta G^{\ddagger}_{rac}$ of 23.8 kcal/mol.[5]

The racemization path for **3** at the B3LYP/6-31G(d) level is a bit more complex and is illustrated in Figure 3. In this case, the C_{2h} structure is not an intermediate but a slight transition state (TS2) connecting enantiomeric C_2-symmetric intermediates (INT and eINT). TS2 is merely the low barrier for counter-rotation of the two central phenyl groups in INT (about the bonds designated by solid atoms in Fig. 2). The chemically significant barrier to racemization is again provided by a C_1-symmetric TS1 that is 33.2 kcal/mol above the D_2 GS. In terms of conformational changes, TS1 is rather 'late': in order to reach the transition state structure, benzo group A (see Fig. 2) has largely moved past the face of the adjacent phenyl ring, and benzo B is in the process of slipping by its neighboring phenyl.

The calculated relative free energy (ΔG=33.2 kcal/mol) for TS1 is significantly higher than the experimental $\Delta G^{\ddagger}_{rac}$ for **3**. As noted before, we have observed that B3LYP/6-31G(d) tends to overestimate the barriers in conformational reactions of complex aromatic molecules,[17] but this discrepancy (9.4 kcal/mol) is unusually large. GAUSSIAN 03[18] frequency calculations provide several measures for comparing the relative energies of minima and transition states, but the two most useful are (a) the zero-point-corrected energy and (b) the free energy (that contains both zero-point and thermal corrections). When these are used to compile tables of *relative* energies and *relative* free energies (ΔE_{corr} and ΔG_{298}, Table 1), the two values rarely differ by more than 1 kcal/mol for conformational reactions. Interestingly, in the case of TS1 for **3**, ΔE_{corr} (30.6 kcal/mol) is rather lower than ΔG_{298} (33.2 kcal/mol), although still higher than the experimental value.

The TS1 structure is very similar to the AM1 transition state structure[5] for this process (that *is* in close agreement with the experimental $\Delta G^{\ddagger}_{rac}$), but there remains the possibility of an alternate pathway for the racemization of **3**. For example, there exists a C_2-symmetric structure for compound **3** that is analogous to INT1 for compound **2**; this minimum is 20.7 kcal/mol above the GS at the B3LYP/6-31G(d) level of theory. However, we have so far been unable to locate any path for the racemization of **3** that proceeds through this C_2 intermediate. If one exists, it may be even more complex than the enantiomerization pathway for compound **2**, but not necessarily lower in energy than the path illustrated in Figure 3.

2.4. Phenyl rotations in compounds 1–3

Besides twist inversion the only other conformational reactions of compounds **1**–**3** are the rotations of phenyl groups. Transition

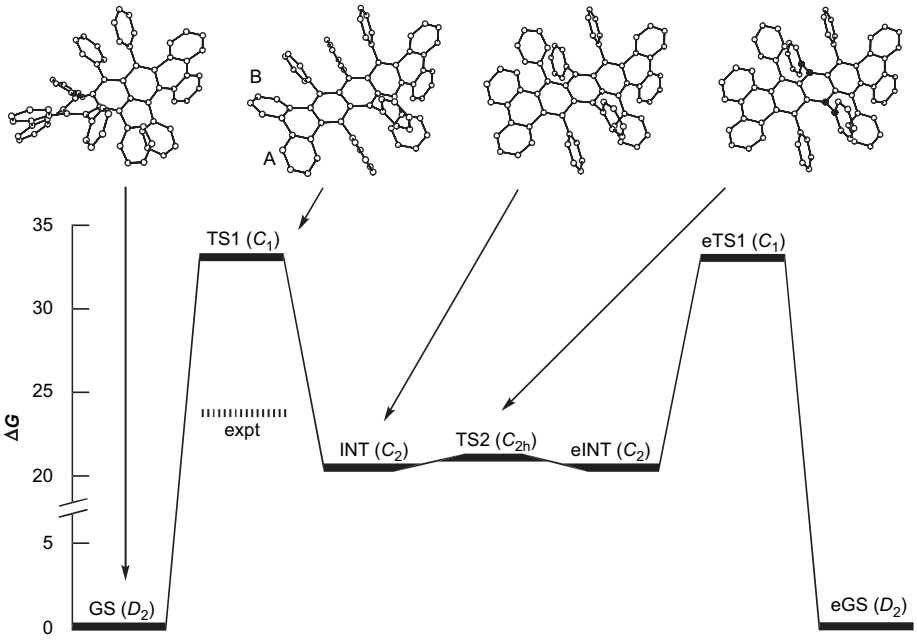

Figure 3. Free energy profile for the twist inversion of 9,10,11,20,21,22-hexaphenyltetrabenzo[*a*,*c*,*l*,*n*]pentacene (**3**) calculated at the B3LYP/6-31G(d) level of theory. The ball-and-stick drawings illustrate the potential minima and transition state structures for this process.

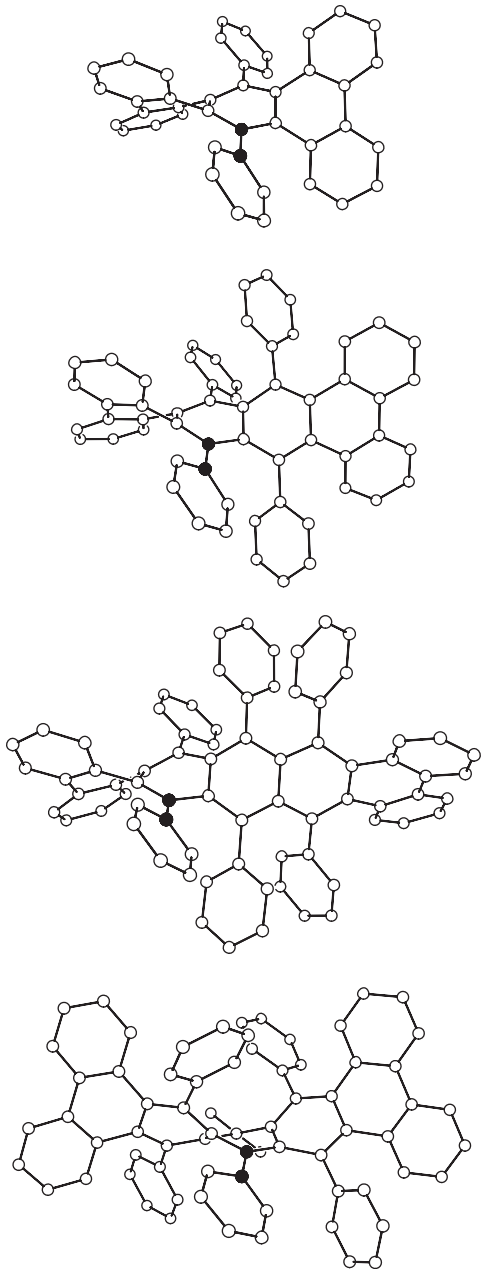

Figure 4. B3LYP/6-31G(d)-calculated high-energy transition state structures for the phenyl rotations in compounds **1**–**3**. The solid atoms highlight the bonds about which the rotations occur.

states for these processes are well defined and easily located, and they are illustrated in Figure 4. In each case the phenyl rotation causes the acene core of the molecule to increase substantially in twist. Thus, the B3LYP/6-31G(d)-calculated end-to-end twist of the GS conformation of **1** is 71.5°, but in the C_2-symmetric phenyl rotation TS structure, the twist is 97.1°, an increase of 25.6°. Similarly, in the phenyl rotation TS for **2**, the twist increases by 25.4°, in the 'side' phenyl rotation TS for **3**, by 26.8°, and in the central phenyl rotation TS for **3**, by 11.4° (along with substantial bending of the pentacene core).

These phenyl rotation TS structures 'look just as one would expect', in contrast to the rather counterintuitive racemization TS structures discussed previously. Instead, it is the calculated relative free energies of the rotation transition states (Table 1) that are unexpected: 36.7 kcal/mol for **1**, 36.5 kcal/mol for **2**, and 37.0 and 35.5 kcal/mol for **3**. These values are *much* higher than the experimental values for phenyl rotations in simple hexaarylbenzenes (17–18 kcal/mol[19–21]) and comparable to the barriers observed for the rotation of *ortho*-tolyl groups in crowded hexaarylbenzenes and octaarylnaphthalenes (33–38 kcal/mol[19,20,22]). To be sure, the resistance provided by the spring-like twisted acene cores of **1**–**3** might give rise to such high barriers, but there is no experimental measurement for any of these processes. In addition, there is always the possibility that a stepwise pathway for the rotation may operate. For example, the phenyl rotation barrier in the 'slice' conformation of **1** (Table 1; illustrated in Section 2.1) cannot be very high, but one or more high-energy steps may be required to reach this conformation, itself 22 kcal/mol above the GS. For this reason, some experimental data bearing on the phenyl rotations is desirable.

The best candidate for such a measurement, in terms of both synthesis and analysis, is compound **6** (Scheme 1) in which the phenyl groups of **3** have been replaced by *m*-(trifluoromethyl)phenyls. The CF_3s are located so that they do not interfere with aryl rotation, but they are large enough that chromatographic separation of the resulting cis and trans isomers of **6** might be possible, and CF_3s are excellent reporter groups for ^{19}F NMR spectroscopy.

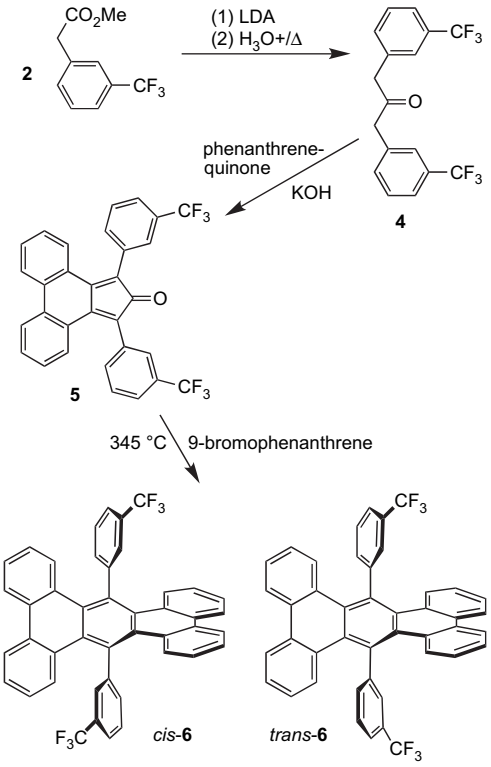

Scheme 1.

Compound **6** was synthesized in the usual manner for derivatives of **1**.[3] The CF_3-substituted diphenylacetone **4** was prepared from the commercially available ester, and **4** was condensed with phenanthrenequinone to give cyclopentadienone **5**. Pyrolysis of **5**, mixed with a bit of 9-bromophenanthrene for 'solvent', at 345 °C gave **6** as a golden crystalline solid in 54% yield.

The ^{19}F NMR spectrum of **6** shows two closely spaced resonances in a 1:1 ratio for the cis and trans isomers, the expected equilibrium mixture generated by a high temperature synthesis. Unfortunately, chromatographic trials on a variety of supports failed to resolve the mixture, so an estimation of the rotation barrier by the thermal isomerization of one of the isomers was not possible. However,

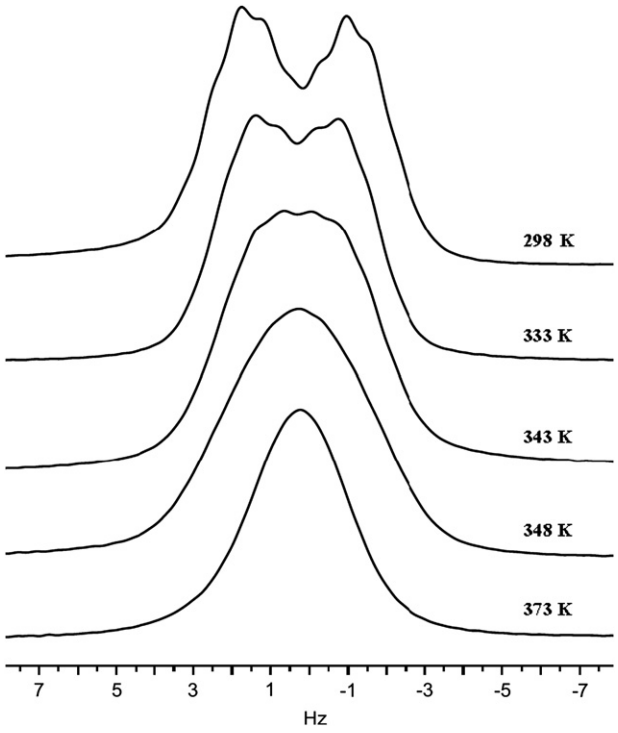

Figure 5. Variable temperature ^{19}F NMR spectrum (376 MHz, toluene-d_8) of compound **6**. The small ripples in the lower temperature spectra are due to long-range ^{1}H–^{19}F spin–spin coupling.

NMR spectroscopy of **6** can provide a lower limit for the barrier to aryl rotation. The fact that two close ^{19}F resonances ($\Delta\nu$=3 Hz at 376 MHz) are observed for **6** in toluene-d_8 at room temperature is already an indication that the barrier is at least 16 kcal/mol. It was most surprising to find, however, that coalescence of these resonances occurred at a mere 75 °C (see Fig. 5), indicating that the barrier to aryl rotation is only 19.2 kcal/mol (from the Gutowsky–Holm approximation, k_c=6.7 s^{-1} is at T_c=348 K, and assuming a transmission coefficient of 1 for the Eyring equation).

Given the 17 kcal/mol discrepancy between the calculated and experimental $\Delta G^{\ddagger}_{rot}$s for **1**, it is clear that phenyl rotation in **1** cannot be the reaction defined by the TS illustrated in Figure 4. After an additional round of computational searches, a remarkable TS was discovered for a concerted phenyl rotation and twist inversion, and this new reaction profile is illustrated in Figure 6. In this process, as the phenyl rotation begins, the phenyl group moves 'above' the polycyclic core, which simultaneously begins to flatten. In the TS, which possesses C_s symmetry, the phenyl group is exactly half rotated, and the two benzo groups on the opposite side of the molecule are in the midst of slipping past the non-rotating phenyl group in opposite directions. This new TS is only 21.4 kcal/mol above the GS, in good agreement with the experimental $\Delta G^{\ddagger}_{rot}$ for compound **6**. It is important to note that, although this reaction also results in twist inversion, this has no experimental consequence for the racemization barrier, because a lower energy pathway for racemization exists.

In light of these experimental and computational results, it is fair to question the chemical relevance of the high-energy phenyl rotation transition states for compounds **2** and **3**. Although we have not conducted searches for alternate phenyl rotation transition states in **2** and **3**, it is obvious that a phenyl rotation in INT2 for the inversion of **2** (Fig. 2) might be relatively easy, and similar structures for compound **3**, if they exist, might provide lower energy pathways for phenyl rotations in that molecule. On the other hand, **2** and **3** are even more tightly twisted molecules than **1**, and a low-energy pathway for concerted twist inversion and one or more ring inversions, as was found for **1**, is extremely unlikely. From an experimental perspective, both the synthesis and NMR analysis of labeled versions of **2** and **3** would be more complicated than for **1**, because of the proliferation of cis and trans diastereomers, to a greater or lesser degree, depending on the labeling scheme. We happily leave such a task to the interested reader.

3. Conclusion

The exceptional chiroptical properties of resolved twisted acenes[4,5,23] (e.g., for **3**, $[\alpha]_D^{25}$=7400°) make them interesting candidates for some materials applications, but only if the

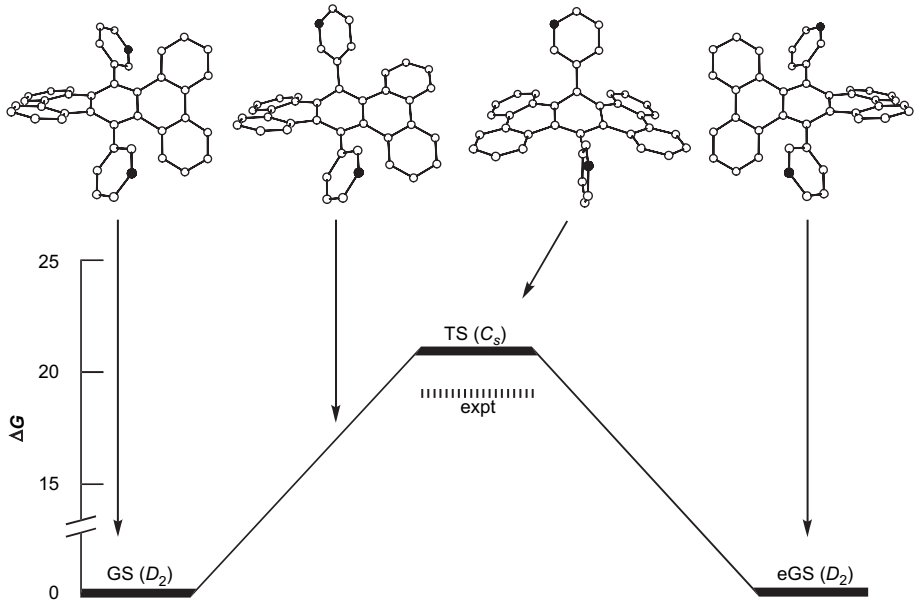

Figure 6. Free energy profile for concerted phenyl rotation and twist inversion in 9,18-diphenyltetrabenz[*a,c,h,j*]anthracene (**1**) calculated at the B3LYP/6-31G(d) level of theory. The ball-and-stick drawings illustrate the potential minima and transition state structure for this process, as well as a transitional structure that is not a stationary point, but which helps to illustrate the process. The solid atoms highlight the trans–cis isomerization that was observed experimentally.

configurational stability can be improved. Unfortunately, the conformational complexity of these molecules, as revealed by the present study, makes it difficult to say that any particular structural modification will ensure configurational stability. Even for the simplest compound (**1**), three separate racemization transition states have been identified, and the situation is not necessarily less complex for **2** and **3**. The fact that compound **3** has a higher experimental barrier to racemization than **1** makes it tempting to say that an even longer twisted acene should be configurationally stable. However, since racemization is a multistep process in the larger twisted acenes, at some point increasing the length may cease to have a significant effect on the barriers for the individual steps, even though they may be more numerous.

These studies also serve as a reminder (if one was needed) that computational predictions must be tested by experiment whenever possible. The high-energy phenyl rotation transition states identified here are *genuine* transition states, but they are not necessarily the *only* transition states for phenyl rotation, as was revealed by the experimental rotation barrier determination. Thus the calculations provide possibilities and insights for structures and mechanisms, but only by comparison of the computational barriers with experimental barriers can one have confidence that the calculated transition states and TS structures are chemically relevant. When they do agree, however, the calculated TS structures provide windows into the reactions that cannot be obtained in any other way.

4. Experimental

4.1. Data for compounds

*4.1.1. 1,3-Bis[3-(trifluoromethyl)phenyl]acetone (**4**)*

A solution of *n*-butyllithium (6.9 mL of a 2.5 M solution in hexanes, 17.2 mmol) was added to a solution of diisopropylamine (2.43 mL, 17.2 mmol) in ether (40 mL) at 0 °C. Methyl 3-trifluoromethylphenylacetate (2.25 g, 11.5 mmol) was slowly added, and the enolate solution was stirred for 30 min. A second equivalent of the ester (2.25 g, 11.5 mmol) was added, the ice bath was removed, and stirring was continued for 16 h at room temperature. The reaction mixture was poured into 1 M HCl (50 mL) and it was extracted with ether (3×50 mL). The combined extracts were washed with water, dried over Na_2SO_4, and concentrated to give an orange oil. This material was taken up in acetic acid (50 mL) and 6 M HCl (10 mL), and the solution was heated at reflux for 8 h. Heating was discontinued, the solvent was removed, and the residue was dissolved in ether (200 mL). The solution was washed with water and satd $NaHCO_3$, and dried over Na_2SO_4. Concentration left a light orange oil that deposited white needles of pure compound **4** (2.78 g, 8.03 mmol, 70%): mp 48–49 °C; ^{1}H NMR ($CDCl_3$) δ 3.84 (s, 4H), 7.34 (d, J=7.5 Hz, 2H), 7.39 (s, 2H), 7.44 (t, J=7.5 Hz, 2H), 7.54 (d, J=7.5 Hz, 2H); ^{13}C NMR ($CDCl_3$) δ 48.9, 123.9 (q, J_{CF}=272 Hz), 124.2 (q, J_{CF}=4 Hz), 126.3 (q, J_{CF}=4 Hz), 129.2, 131.1 (q, J_{CF}=32 Hz), 132.9, 134.3, 203.7 (9 of 9 expected resonances observed); MS (EI) m/z 346 (M^+, 3), 327 (M−F, 4), 187 (M−$CF_3C_6H_4CH_2$, 19), 159 ($CF_3C_6H_4CH_2^+$, 100); exact mass (ESI) 346.0794, calcd for $C_{17}H_{12}OF_6$ 346.0792.

*4.1.2. 1,3-Bis[3-(trifluoromethyl)phenyl]cyclopenta[l]phenanthren-2-one (**5**)*

Phenanthrenequinone (0.287 g, 1.38 mmol) was added to a solution of compound **4** (0.478 g, 1.38 mmol) in ethanol (10 mL). KOH (four drops of a 20% solution in EtOH) was added at room temperature, the quinone dissolved, and the reaction mixture was then immediately immersed in a boiling water bath with constant swirling. An additional four drops of KOH solution were added, and, after heating for 3 min (at which point the solution was boiling), the reaction mixture was chilled in an ice bath with constant swirling for 7 min. Dark green crystals of compound **5** were collected by filtration (0.18 g, 0.35 mmol, 25%): mp 207–215 °C (dec); ^{1}H NMR ($CDCl_3$) δ 6.99 (td, J=8, 1 Hz, 2H), 7.34 (td, J=8, 1 Hz, 2H), 7.46 (dd, J=8, 1 Hz, 2H), 7.59 (m, 4H), 7.65 (d, J=8 Hz, 2H), 7.69 (s, 2H), 7.85 (d, J=8 Hz, 2H); ^{13}C NMR ($CDCl_3$) δ 121.7, 123.3, 124.8, 125.0 (q, J_{CF}=4 Hz), 126.1 (q, J_{CF}=4 Hz), 126.9 (q, J_{CF}=4 Hz), 127.1, 127.7, 127.8, 128.0, 128.5, 128.6, 128.9, 129.2, 129.4, 130.4 (q, J_{CF}=4 Hz), 130.8, 131.2 (q, J_{CF}=33 Hz), 131.6, 132.2, 132.8, 133.4, 133.7, 133.8, 135.1, 138.0, 149.4, 197.1, 199.0 (29 of 32 expected resonances observed for a mixture of cis and trans isomers; the two CF_3s and one of the attached quaternary C's were not observed); exact mass (ESI) 518.1106, calcd for $C_{31}H_{16}OF_6$ 518.1105.

*4.1.3. 9,18-Bis[3-(trifluoromethyl)phenyl]tetrabenz[a,c,h,j]anthracene (**6**)*

Compound **5** (160 mg, 0.309 mmol) and 9-bromophenanthrene (79 mg, 0.31 mmol) were mixed in a Pyrex screw-capped tube and heated at 345 °C for 1 h. After cooling, the resulting black solid was chromatographed on a silica gel column eluted with 25:1 hexanes–benzene. The desired product (R_f 0.6 by TLC in 2:1 hexanes–benzene) eluted as a yellow band. Concentration of these fractions yielded pure compound **6** as a yellow crystalline solid (55 mg, 0.083 mmol, 54%): mp 279–283 °C; ^{1}H NMR ($CDCl_3$) δ 7.00 (m, 6H), 7.07 (d, J=8 Hz, 2H), 7.43 (m, 4H), 7.50 (t, J=8 Hz, 2H), 7.64 (m, 2H), 7.69 (d, J=8 Hz, 2H), 7.73 (m, 2H), 8.40 (t, J=8 Hz, 4H); ^{19}F NMR ($CDCl_3$) δ −63.11, −63.10; ^{19}F NMR (toluene-d_8) δ −62.83, −62.82; MS (EI) m/z 666 (M^+, 100), 647 (M−F, 2); exact mass (ESI) 666.1772, calcd for $C_{44}H_{24}F_6$ 666.1782.

4.2. General computational methods

All semiempirical (AM1[11]) and density functional [B3LYP/6-31G(d)[13,14]] calculations were performed by using GAUSSIAN 03,[18] and its default thresholds for wave function and gradient convergence were employed. Transition states were located by means of quadratic synchronous transit algorithms (QST2 and QST3 program options) or by optimization under a symmetry constraint. All potential minima and transition states were verified by analytical frequency calculations. For a more detailed discussion of the strategies employed to locate conformational transition states in a very large, symmetric hydrocarbon, see Ref. 17.

Acknowledgements

This work was supported by National Science Foundation Grant CHE-0614879, and it is gratefully acknowledged.

Supplementary data

It consists of a PDF file containing a table of the calculated *absolute* energies (E), zero-point-corrected energies (E+*ZPE*), and free energies (G_{298}) for the structures calculated in this study, and an ASCII text file containing the atomic coordinates of the minimum and transition state structures calculated at the B3LYP/6-31G(d) level. Supplementary data associated with this article can be found in the online version, at doi:10.1016/j.tet.2008.05.030.

References and notes

1. Review: Pascal, R. A., Jr. *Chem. Rev.* **2006**, *106*, 4809–4819.
2. Pascal, R. A., Jr.; McMillan, W. D.; Van Engen, D. *J. Am. Chem. Soc.* **1986**, *108*, 5652–5653.
3. Pascal, R. A., Jr.; McMillan, W. D.; Van Engen, D.; Eason, R. G. *J. Am. Chem. Soc.* **1987**, *109*, 4660–4665.
4. Lu, J.; Ho, D. M.; Vogelaar, N. J.; Kraml, C. M.; Pascal, R. A., Jr. *J. Am. Chem. Soc.* **2004**, *126*, 11168–11169.
5. Lu, J.; Ho, D. M.; Vogelaar, N. J.; Kraml, C. M.; Bernhard, S.; Byrne, N.; Kim, L. R.; Pascal, R. A., Jr. *J. Am. Chem. Soc.* **2006**, *128*, 17043–17050.
6. Norton, J. E.; Houk, K. N. *J. Am. Chem. Soc.* **2005**, *127*, 4162–4163.

7. Smyth, N.; Van Engen, D.; Pascal, R. A., Jr. *J. Org. Chem.* **1990**, *55*, 1937–1940.
8. Meurer, K. P.; Vogtle, F. *Top. Curr. Chem.* **1985**, *127*, 1–76.
9. Clark, M.; Cramer, R. D., III; Van Opdenbosch, N. *J. Comput. Chem.* **1989**, *10*, 982–1012.
10. Halgren, T. A. *J. Comput. Chem.* **1996**, *17*, 490–519.
11. Dewar, M. J. S.; Zoebisch, E. G.; Healy, E. F.; Stewart, J. J. P. *J. Am. Chem. Soc.* **1985**, *107*, 3902–3909.
12. Hehre, W. J.; Radom, L.; Schleyer, P. v. R.; Pople, J. A. *Ab Initio Molecular Orbital Theory*; John Wiley & Sons: New York, NY, 1986, pp 133–226.
13. Becke, A. D. *J. Chem. Phys.* **1993**, *98*, 5648–5652.
14. Lee, C.; Yang, W.; Parr, R. G. *Phys. Rev. B* **1988**, *37*, 785–789.
15. The energies quoted in the text and plotted in Figures 1–3 and 6 are the calculated relative free energies (ΔG_{298}) of the structures under discussion. The relative energies (ΔE) and zero-point-corrected energies (ΔE_{corr}), which are generally similar, may be found in Table 1 for comparison.
16. Bock, H.; Havlas, Z.; Gharagozloo-Hubmann, K.; Sievert, M. *Angew. Chem., Int. Ed.* **1999**, *38*, 2240–2243.
17. Pascal, R. A., Jr.; Kraml, C. M.; Byrne, N.; Coughlin, F. J. *Tetrahedron* **2007**, *63*, 11902–11910.
18. Frisch, M. J.; Trucks, G. W.; Schlegel, H. B.; Scuseria, G. E.; Robb, M. A.; Cheeseman, J. R.; Montgomery, J. A., Jr.; Vreven, T.; Kudin, K. N.; Burant, J. C.; Millam, J. M.; Iyengar, S. S.; Tomasi, J.; Barone, V.; Mennucci, B.; Cossi, M.; Scalmani, G.; Rega, N.; Petersson, G. A.; Nakatsuji, H.; Hada, M.; Ehara, M.; Toyota, K.; Fukuda, R.; Hasegawa, J.; Ishida, M.; Nakajima, T.; Honda, Y.; Kitao, O.; Nakai, H.; Klene, M.; Li, X.; Knox, J. E.; Hratchian, H. P.; Cross, J. B.; Bakken, V.; Adamo, C.; Jaramillo, J.; Gomperts, R.; Stratmann, R. E.; Yazyev, O.; Austin, A. J.; Cammi, R.; Pomelli, C.; Ochterski, J. W.; Ayala, P. Y.; Morokuma, K.; Voth, G. A.; Salvador, P.; Dannenberg, J. J.; Zakrzewski, V. G.; Dapprich, S.; Daniels, A. D.; Strain, M. C.; Farkas, O.; Malick, D. K.; Rabuck, A. D.; Raghavachari, K.; Foresman, J. B.; Ortiz, J. V.; Cui, Q.; Baboul, A. G.; Clifford, S.; Cioslowski, J.; Stefanov, B. B.; Liu, G.; Liashenko, A.; Piskorz, P.; Komaromi, I.; Martin, R. L.; Fox, D. J.; Keith, T.; Al-Laham, M. A.; Peng, C. Y.; Nanayakkara, A.; Challacombe, M.; Gill, P. M. W.; Johnson, B.; Chen, W.; Wong, M. W.; Gonzalez, C.; Pople, J. A. *Gaussian 03, Revision C.02*; Gaussian: Wallingford, CT, 2004.
19. Gust, D. *J. Am. Chem. Soc.* **1977**, *99*, 6980–6982.
20. Gust, D.; Patton, A. *J. Am. Chem. Soc.* **1978**, *100*, 8175–8181.
21. Komber, H.; Stumpe, K.; Voit, B. *Tetrahedron Lett.* **2007**, *48*, 2655–2659.
22. Qiao, X.; Pelczer, I.; Pascal, R. A., Jr. *Chirality* **1998**, *10*, 154–158.
23. At the request of a referee, the specific rotations of the D_2 ground states of compounds **1**–**3** were calculated at the B3LYP/6-31G(d) level (using the dipole electric field polarizabilities), yielding $[\alpha]_D$=559°, 460°, and 1737°, respectively. The last is obviously much lower than the experimentally determined value of 7400° for **3**.